

Solid-source molecular-beam epitaxy growth of GaInNAsSb/InGaAs single quantum well on InP with photoluminescence peak wavelength at 2.04 μm

Jun-Xian Fu^{a)}

Department of Applied Physics, Stanford University, Stanford, California 94305

Seth R. Bank, Mark A. Wistey, Homan B. Yuen, and James S. Harris, Jr.

Solid State and Photonics Laboratory, Stanford University, Stanford, California 94305

(Received 27 October 2003; accepted 10 February 2004; published 8 June 2004)

Single quantum wells $\text{In}_{0.53}\text{Ga}_{0.47}\text{As}/\text{Ga}_{0.47}\text{In}_{0.53}\text{N}_{0.021}\text{As}_{0.949}\text{Sb}_{0.03}/\text{In}_{0.53}\text{Ga}_{0.47}\text{As}$ with room-temperature photoluminescence peak wavelength at 2.04 μm were grown on InP substrate by solid-source molecular-beam epitaxy (MBE). *In situ* reflection high-energy electron diffraction was used to monitor the MBE growth. Double-crystal high-resolution x-ray diffraction and secondary ion mass spectrometry were utilized to characterize the samples and optimize the growth conditions. The roles of nitrogen and antimony atoms in the growth of quinary material, GaInNAsSb, were investigated. © 2004 American Vacuum Society. [DOI: 10.1116/1.1691411]

I. INTRODUCTION

GaInNAs/GaAs has been extensively studied as a substitute material system for InGaAsP/InP in the pursuit of lower cost and more efficient lasers in optical communication.^{1–3} There were several theories explaining the mechanisms of band-gap narrowing for nitrogen incorporation in GaAsN or GaInNAs.^{4–9} With additional antimony atoms incorporated in the active region, the crystal and optical quality of a dilute nitride layer can be significantly improved and the operating wavelength can be pushed further from 1.3 μm to 1.55 μm which covers the entire *S–C–L* bands of long-haul optical communications.^{10,11}

Low-noise near-infrared photodetectors within the wavelength range of 2–2.5 μm are of great interest to biosensing (e.g., noninvasive blood glucose analysis) and environmental gas detection. Since lead–salt detectors and extended InGaAs detectors have unsatisfactory dark-current performance at room temperature, integrated systems using other materials operating in this wavelength range with better performance are required. Integration of the photodetector, light source, and circuits on the same semiconductor substrate cannot only reduce the overall cost, but also increase the performance of the system response. Lattice-matched GaInNAs grown on an InP substrate has the potential to reach this wavelength region with the introduction of only several percent nitrogen.^{12,13}

In this article, we report the growth of GaInNAsSb on an InP substrate by solid-source molecular-beam epitaxy (MBE) equipped with a nitrogen plasma source with a room-temperature photoluminescence (PL) peak at 2.04 μm . *In situ* reflective high-energy electron diffraction (RHEED) was used to observe the surface reconstruction and monitor the epitaxial layer growth. High-resolution x-ray diffraction (HRXRD), secondary ion mass spectrometry (SIMS), and

room-temperature PL were utilized to characterize the material quality and optimize the crystal growth condition. The correlation of indium atoms and nitrogen atoms during the growth of GaInNAs(Sb) was analyzed by SIMS. Group-III growth rate dependent and antimony-enhanced nitrogen incorporation mechanisms were deduced from HRXRD measurement and SIMS analysis. After-growth annealing and room-temperature PL were investigated for InGaAs/GaInNAs(Sb)/InGaAs samples.

II. EXPERIMENT

The samples were grown in a Varian Gen-II MBE system with indium and gallium SUMO cells from Applied Epi. By controlling the temperature of the tip and base zones of the cells, stable source flux are obtained so that during growth the lattice match condition can be maintained. The arsenic source was a precisely controlled needle-valve cracker with the sublimation region set to 390 °C and the cracking zone set to 800 °C. The antimony source was a nonvalved cell with two heating zones at idle temperature when not used. During epitaxial layer growth, the flux of arsenic was monitored by the needle-valve position, and the flux of antimony was controlled by the sublimation zone temperature (450–490 °C) while the cracking zone temperature was 850 °C. The nitrogen source is a modified SVT plasma source with the highest rf power of 300 W and ultraclean nitrogen gas flow up to 5 sccm.

The desorbing temperature of phosphorous from InP substrate is around 300 °C, while the oxide layer on the surface remains untouched until InP decomposes at a temperature of around 500 °C.¹⁴ The oxide blowoff process varies based the substrate history and blowoff environment.¹⁵ The substrate was first heated quickly to 300 °C without arsenic overpressure. Then, in an arsenic overpressure environment, the substrate was heated to 350 °C and ramped to 510 °C with ramping rate of 20 °C/min in an arsenic beam equivalent pressure (BEP) flux of 10^{-6} Torr. After a 2×4 surface reconstruction

^{a)}Author to whom correspondence should be addressed; electronic mail: junxian@stanford.edu

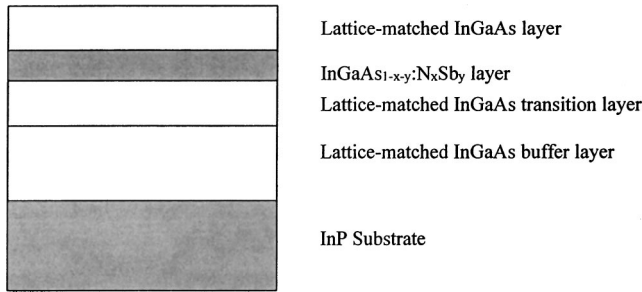


Fig. 1. Sample structure: Substrate was $n+(100)$ InP, buffer layer was 200–300 nm InGaAs lattice matched to InP with strain less than 8×10^{-4} , transition layer of lattice-matched InGaAs has a thickness of 100 nm, thin layer of InGaAs_{1-x-y}N_xSb_y has a thickness of 20–50 nm, cladding and capping layer of InGaAs is 80–150 nm.

is clearly recognized, the substrate was cooled to 370–390 °C and lattice-matched In_{0.53}Ga_{0.47}As buffer layer was grown with a mismatch strain of less than 0.05%, followed by a GaInNAsSb layer growth.

The structure of the samples grown in this study is shown in Fig. 1. The capping layer, the cladding layer, and the buffer layer were lattice-matched In_{0.53}Ga_{0.47}As layers directly grown on InP substrate. The thickness of the thin layer of Ga_{0.47}In_{0.53}N_xAs_{1-x-y}Sb_y is between 20 nm and 50 nm. As shown in Fig. 1, after the buffer layer growth, the transition layer of lattice-matched InGaAs was grown with substrate temperature gradually cooled down to 370–390 °C and the nitrogen plasma was ignited 10–15 min before the growth of the single quantum well (SQW) layer. The use of a transition layer can reduce nonradiative defects in the SQW layer when the substrate temperature changes during the growth of the cladding layer and SQW layer. The background N level at a growth rate of 0.5 $\mu\text{m/h}$ was around 0.15%. During the growth of the SQW layer, N and Sb shutters were opened and 20–50 nm InGaAsNSb layers were grown. A capping layer of a lattice-matched InGaAs layer was grown on the top of the SQW layer.

III. RESULTS AND DISCUSSION

In this study, three samples were grown and studied. For sample 1, the indium source had a BEP flux of 1.42×10^{-7} Torr (corresponding to a growth rate of 0.167 $\mu\text{m/h}$); the gallium source had a BEP flux of 8.80×10^{-8} Torr (growth rate of 0.148 $\mu\text{m/h}$); the antimony BEP flux was 5.88×10^{-8} Torr and the arsenic BEP flux 3.5×10^{-6} Torr; the thickness of GaInNAsSb layer (group-III dependent only) was 50 nm and the cladding and capping layer thicknesses were 150 nm. For samples 2 and 3, the BEP flux was 2.20×10^{-7} Torr (growth rate of 0.257 $\mu\text{m/h}$) for indium source and 1.36×10^{-7} Torr (growth rate of 0.228 $\mu\text{m/h}$) for the gallium source; the antimony BEP flux was 7.68×10^{-8} Torr and the arsenic BEP flux 5.4×10^{-6} Torr; the thicknesses of both GaInNAs (sample 2) and GaInNAsSb (sample 3) layers were 20 nm and the cladding and capping layer thicknesses were 80 nm. The nitrogen flow (10% of 5

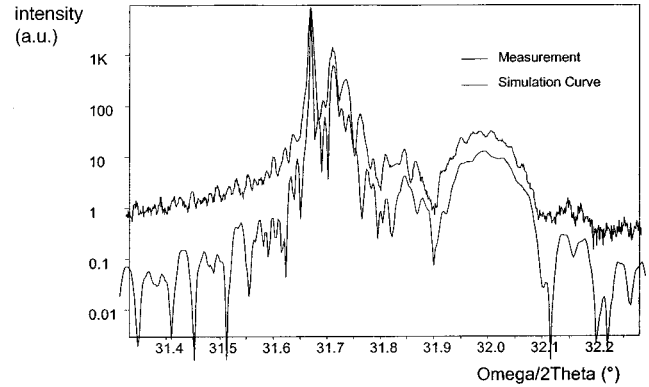


Fig. 2. HRXRD measurement of sample 1: SQW layer of 50 nm, simulation curve shows one possible combination of N with 3.5% and Sb with 3.0%.

scm) and the rf power (300 W) were kept the same for all three samples. The ratio of BEP(As)/BEP(In+Ga) was between 15 and 20.

A. N and Sb composition analysis

Although the solubility of nitrogen atoms in semiconductor bulk materials was theoretically expected to be very low, Tu and co-workers¹⁶ found that up to 14.8% N can be incorporated in GaAsN layers without phase segregation. Due to the different bond strength of InNAs and GaNAs, phase separation was expected for a high nitrogen concentration or unoptimized growth conditions. To avoid phase separation, a low growth temperature to provide metastable growth has to be used for nitride layers. The growth temperature unfortunately forms extra defects that can be significantly reduced by after-growth annealing (discussed later). Nitride layers with a relatively high concentration of nitrogen can be grown using a lower growth rate.

HRXRD simulation of sample 1 (Fig. 2) and SIMS analysis (Fig. 3) show that up to 3.5% N and 3% Sb can be incorporated into the nearly lattice-matched InGaAs layers to form a 50 nm Ga_{0.47}In_{0.53}N_{0.035}As_{0.935}Sb_{0.03} layer, which has a tensile strain of 0.9%. No evidence of phase separation (GaN, InN, GaAs, InAs, GaSb, or InSb) can be found in the wider omega scan (not shown) in the HRXRD measurement.

It has been found that the N composition (N%) is reciprocally proportional to the growth rate (g , in $\mu\text{m/h}$) of group III (In+Ga) for MBE growth of GaInNAs on GaAs,¹⁷

$$N\% = \frac{A}{g_{\text{In}} + g_{\text{Ga}}} \quad (1)$$

A best fit of different samples with various growth conditions leads to a nitrogen incorporation factor $A \sim 1.0$.

It is well known that antimony atoms act as a surfactant when they were added to a GaInNAs layer growth to form a layer of GaInNAsSb. These layers have smoother surfaces, fewer defects, and better crystalline and optical quality than GaInNAs layers.¹⁸ During the growth of samples 2 and 3, the RHEED pattern shows that nitrogen atoms roughen the layer surface while additional antimony atoms make the layer surface smoother. HRXRD measurements of samples 2 and 3

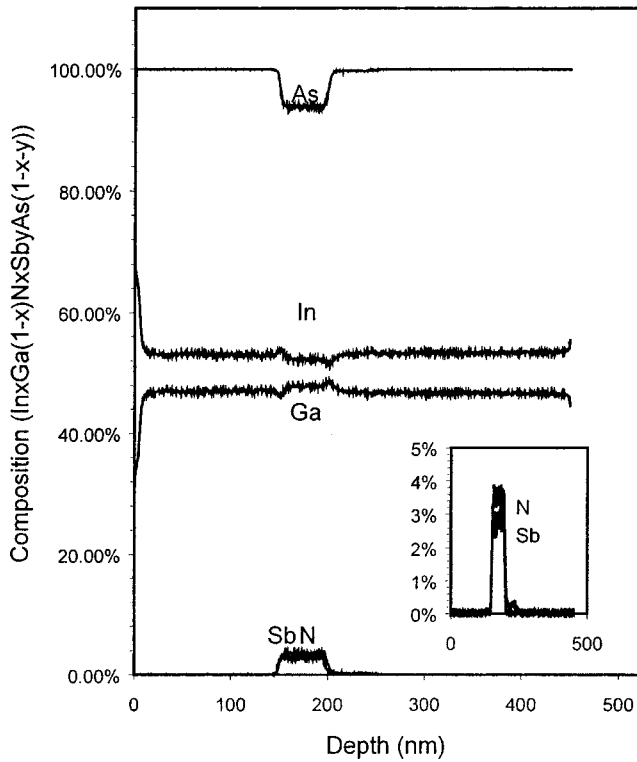


FIG. 3. SIMS analysis of sample 1, inset shows the N and Sb concentration. The raw data (not shown) of In show that thin InGaAsNSb layer has 3.5% less ion count than that of cladding layer, while there is no such effect of Ga ion count.

show that pendellosung fringes can be clearly recognized away from the peak position (Fig. 4), verifying that antimony atoms incorporated into the thin SQW layer improved the crystalline quality. In addition, antimony atoms partially compensate for the strain induced by the nitrogen atoms (Fig. 4) in the quinary. According to Vegard's law, the lattice-match condition for $\text{Ga}_{0.47}\text{In}_{0.53}\text{N}_x\text{As}_{1-x-y}\text{Sb}_y / \text{In}_{0.53}\text{Ga}_{0.47}\text{As}$ is that $x:y$ equals to 1:2.56. Another role that antimony atoms play in the GaInNAsSb on GaAs layers is that they increase the nitrogen incorporation.^{19,20}

As shown in Fig. 5, with about 3% Sb in the GaInNAsSb layer, the N concentration increases from 1.6% (sample 2) to 2.1% (sample 3). Comparing the results of sample 1 with those of samples 2 and 3, we find that the relationship between the N concentration and group-III growth rate holds precisely for GaInNAs(Sb) growth on InP with one additional factor C_{Sb} ,

$$\text{N}\% = \frac{A \cdot C_{\text{Sb}}}{g_{\text{In}} + g_{\text{Ga}}} \quad (2)$$

The nitrogen incorporation factor for GaInNAs growth on InP is $A \sim 0.8$ and the antimony enhanced factor with Sb concentration of 3.0% $C_{\text{Sb}} = 1.3$.

It was found that the nitrogen composition was independent on indium composition during the MBE growth of GaInNAs layers on a GaAs substrate with In less than 30%.²⁰ However, in the metalorganic vapor phase epitaxy growth of GaInNAs on GaAs,²¹ it was found that the indium

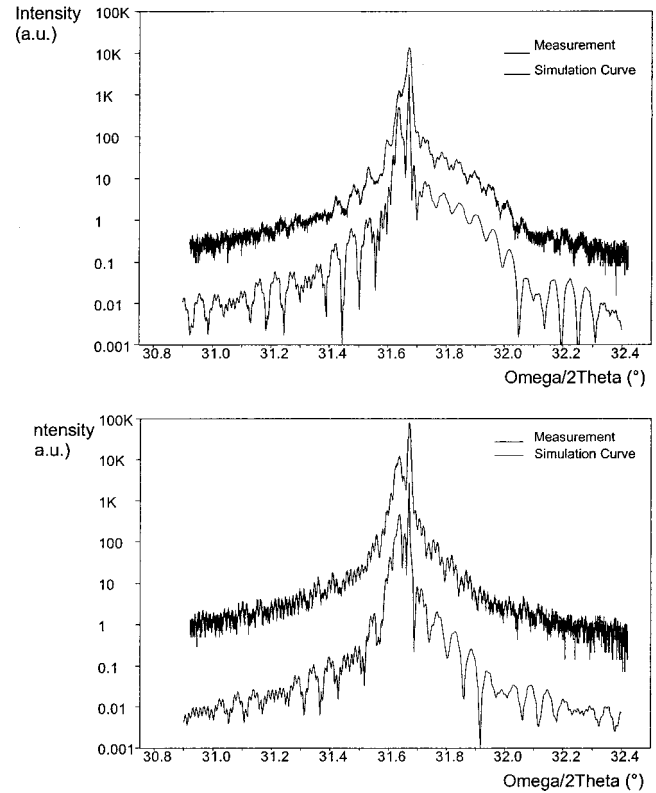


FIG. 4. HRXRD measurement and simulation of sample 2 (SQW layer of GaInNAs with 1.6% N) and sample 3 (SQW layer of GaInNAsSb with one possible combination of 2.1% N and 3.0% Sb).

segregation on the surface changes the surface reconstruction and affects the nitrogen incorporation during the growth. In Fig. 3, the SIMS analysis of sample 1 shows that the indium composition changes in the GaInNAs layer, as well as in the GaInNAsSb layer, compared with the composition in the lattice-matched buffer and cladding layers (see Fig. 6). From the SIMS raw data of analysis, the indium ion count decreased by a certain amount (3.5% in sample 1, 1.5% in sample 2, and 2.1% in sample 3) while no corresponding increase is observed for gallium atoms. Since the indium and gallium source temperatures were precisely controlled not to change during all the layer growths, there must be some intercorrelation of N and In atoms either during the layer growth of GaInNAs(Sb) on InP substrate or in the SIMS analysis. Such an effect should be expected in the growth of GaInNAs(Sb) on GaAs substrate. The cladding layers are either GaAs or GaAsN, thus there is no continuous indium reference. The change of indium concentration is so small that such an effect might have been just overlooked in the past. Moreover, it was unlikely that the ion counting of nitrogen atoms and indium atoms in SIMS were correlated. Therefore, one of the explanations is that nitrogen atoms randomly incorporated in the unit cell of InGaAs statistically change the shape (a mixed state of zinc-blende and wurtzite cell) and the composition of the unit cells. Further theoretical work is needed to investigate the effect of nitrogen atoms on indium atoms during the growth.

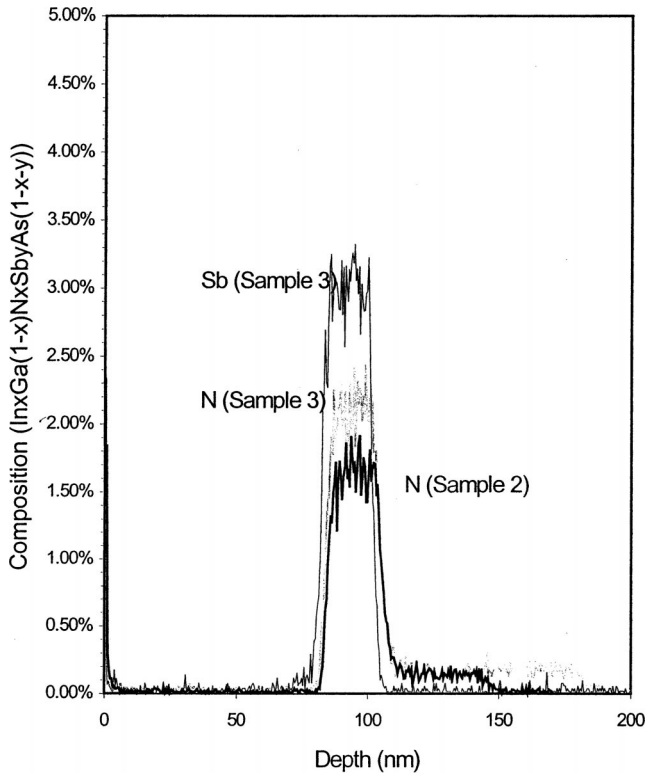


Fig. 5. SIMS analysis of samples 2 and 3: In sample 3, additional Sb atoms increase the likelihood of N incorporation (possibly increasing the sticking coefficient).

B. Sample annealing and photoluminescence measurement

From Figs. 2 and 3 for sample 1, we found that $\text{Ga}_{0.47}\text{In}_{0.53}\text{N}_{0.035}\text{As}_{0.935}\text{Sb}_{0.03}$ grown on $\text{In}_{0.53}\text{Ga}_{0.47}\text{As}$ lattice-matched to InP has an in-plane tensile strain of 0.9%. The theoretically calculated critical thickness for coherent growth is much less than 50 nm. The partially relaxed GaInNAsSb layer has a high concentration of nonradiative defects that quench the PL. Sample 2 has a 20 nm layer of $\text{Ga}_{0.47}\text{In}_{0.53}\text{N}_{0.016}\text{As}_{0.984}$ and sample 3 has a 20 nm layer of

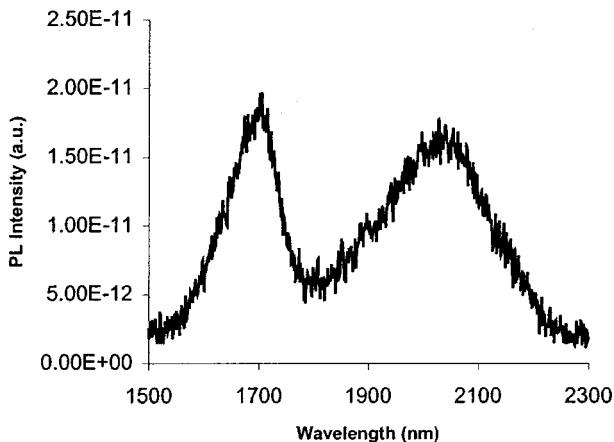


Fig. 6. Room-temperature PL of sample 3: Lattice-matched buffer and cladding layer of InGaAs has a PL peak wavelength at $1.68 \mu\text{m}$, InGaAs $\text{N}_{0.021}\text{Sb}_{0.03}$ layer has a PL peak wavelength at $2.04 \mu\text{m}$.

$\text{Ga}_{0.47}\text{In}_{0.53}\text{N}_{0.021}\text{As}_{0.949}\text{Sb}_{0.03}$ between lattice-matched layers of InGaAs on InP, which are all well within the coherent growth range. After-growth annealing and PL measurement were used to characterize samples 2 and 3.

The low temperature used in the growth of GaInNAs(Sb) introduced extra defects in the layer even with the help of surfactant antimony atoms. After-growth annealing was found to be able to reduce the nonradiative defects formed during nitride layer growth.²² The samples were annealed by rapid thermal annealing with a maximum temperature ramping rate of $200 \text{ }^\circ\text{C/s}$. The optimized annealing condition of GaInNAs(Sb) SQW samples was found to be between $680 \text{ }^\circ\text{C}$ and $720 \text{ }^\circ\text{C}$ for 1 to 10 min.

A luminescence wavelength blueshift of annealed GaInNAs samples was observed similar to that for GaInNAs and GaInNAsSb on GaAs.²¹ This has been both experimentally and theoretically explained by nearest nitrogen neighbors change in GaInNAs/GaAs.²³ But for GaInNAsSb/InP samples, the PL blueshifts under different annealing conditions are not as severe as those of GaInNAs/GaAs samples. One of the possible reasons is that additional antimony atoms in GaInNAsSb/InP reduce the strain compared to increasing the strain in the already highly compressively strained GaInNAsSb QWs on GaAs. This could reduce the driving force for the nearest nitrogen neighbors of GaInNAs samples during annealing. As shown in Fig. 6, the room-temperature PL of sample 3 has a peak wavelength at $2.04 \mu\text{m}$ (corresponding to a band-gap energy of 0.6 eV).

IV. SUMMARY

In summary, InGaAs/GaInNAsSb/InGaAs SQWs with good crystalline and optical qualities have been grown on InP substrates. *In situ* RHEED patterns show that antimony acts as a surfactant when nitrogen is added in MBE growth. HRXRD measurements show that tensile strained GaInNAsSb layers can be grown on lattice-matched InGaAs buffer layers on InP substrates. The nitrogen and antimony compositions are calibrated using HRXRD and SIMS profiling, which show that nitrogen composition is reciprocally proportional to the growth rate of group III (indium and gallium) and that antimony enhances the nitrogen incorporation rate. SIMS analysis also shows that the nitrogen and indium compositions are correlated in the layer growth of GaInNAs(Sb). Rapid thermal annealing reduces the nonradiative defects formed during low-temperature growth of nitride layer. There is less of a blueshift of GaInNAsSb luminescence peak wavelength after annealing compared to similar but most highly strained quinary alloys grown on GaAs. Room-temperature PL was obtained for InGaAs/GaIn $\text{N}_{0.021}\text{As}_{0.949}\text{Sb}_{0.03}$ /InGaAs SQW with PL peak wavelength at $2.04 \mu\text{m}$. The growth of long wavelength material on InP substrate is very useful in developing bio- and chemical gas sensing devices.

ACKNOWLEDGMENTS

The authors gratefully acknowledge Sumitomo Electronics, USA for the InP wafer donation and Charles Evans and

Associates for collaboration on SIMS profiling analysis. The project was funded by DARPA PWASSP project.

- ¹M. Kondow, K. Uomi, A. Niwa, T. Kitatani, S. Watahiki, and Y. Yazawa, *Jpn. J. Appl. Phys., Part 1* **35**, 1273 (1996).
- ²M. Kondow, K. Takeshi, S. Nakatsuka, M. C. Larson, K. Nakahara, Y. Yazawa, M. Okai, and K. Uomi, *IEEE J. Sel. Top. Quantum Electron.* **3**, 719 (1997).
- ³J. S. Harris, Jr., *Semicond. Sci. Technol.* **17**, 880 (2002).
- ⁴W. Shan, W. Walukiewicz, J. W. Ager, E. E. Haller, J. F. Geisz, D. J. Friedman, J. M. Olson, and S. R. Kurtz, *Phys. Rev. Lett.* **82**, 1221 (1999).
- ⁵A. Lindsay and E. P. O'Reilly, *Solid State Commun.* **112**, 443 (1999).
- ⁶W. W. Chow, E. D. Jones, N. A. Modine, A. A. Allerman, and S. R. Kurtz, *Appl. Phys. Lett.* **75**, 2891 (1999).
- ⁷A. Al-Yacoub and L. Bellaiche, *Phys. Rev. B* **62**, 10847 (2000).
- ⁸T. Takayama, M. Yuri, K. Itoh, and J. S. Harris, Jr., *J. Appl. Phys.* **90**, 2358 (2001).
- ⁹P. R. C. Kent, L. Nellaiche, and A. Zunger, *Semicond. Sci. Technol.* **17**, 851 (2002).
- ¹⁰K. Nakahara, M. Kondow, T. Kitatani, M. C. Larson, and K. Uomi, *IEEE Photonics Technol. Lett.* **10**, 487 (1998).
- ¹¹X. Yang, J. B. Heroux, L. F. Mei, and W. I. Wang, *Appl. Phys. Lett.* **78**, 4068 (2001).
- ¹²M. R. Gokhale, J. Wei, H. S. Wang, and S. R. Forrest, *Appl. Phys. Lett.* **74**, 1287 (1999).
- ¹³D. Serries, T. Geppert, P. Ganser, M. Maier, K. Kohler, N. Herres, and J. Wagner, *Appl. Phys. Lett.* **80**, 2448 (2002).
- ¹⁴J. F. Wager, D. L. Ellsworth, S. M. Goodnick, and C. W. Wilmsen, *J. Vac. Sci. Technol. B* **19**, 513 (1981).
- ¹⁵C. Lenox, H. Nie, G. Kinsey, C. Hansing, J. C. Campbell, A. L. Holmes, Jr., and B. G. Streetman, *J. Vac. Sci. Technol. B* **17**, 1175 (1999).
- ¹⁶W. G. Bi and C. W. Tu, *Appl. Phys. Lett.* **70**, 1608 (1997).
- ¹⁷S. G. Spruytte, M. C. Larson, W. Wampler, C. W. Coldren, H. E. Petersen, and J. S. Harris, Jr., *J. Cryst. Growth* **227**, 506 (2001).
- ¹⁸X. Yang, M. J. Jurkovic, J. B. Heroux, and W. I. Wang, *Appl. Phys. Lett.* **75**, 178 (1999).
- ¹⁹F. Dimroth, A. Howard, J. K. Shurtleff, and G. B. Stringfellow, *J. Appl. Phys.* **91**, 3687 (2002).
- ²⁰K. Volz, V. Gambin, W. Ha, M. A. Wistey, H. Yuen, S. Bank, and J. S. Harris, Jr., *J. Cryst. Growth* **251**, 360 (2003).
- ²¹D. J. Friedman, J. F. Geisz, S. R. Hurtz, J. M. Olson, and R. Reedy, *J. Cryst. Growth* **195**, 438 (1998).
- ²²J. F. Geisz, D. J. Friedman, J. M. Olson, S. R. Kurtz, and B. M. Keyes, *J. Cryst. Growth* **195**, 401 (1998).
- ²³V. Lordi, V. Gambin, S. Friedrich, T. Funk, T. Takizawa, K. Uno, and J. S. Harris, Jr., *Phys. Rev. Lett.* **90**, 145505-1 (2003).